Tectonophysics 717 (2017) 413–424

Contents lists available at ScienceDirect

Tectonophysics

journal homepage: www.elsevier.com/locate/tecto

Lg-wave attenuation in the Australian crust

Zhi Wei[a,b,*], Brian L.N. Kennett[c], Lian-Feng Zhao[a]

[a] Key Laboratory of Earth and Planetary Physics, Institute of Geology and Geophysics, Chinese Academy of Sciences, Beijing, China
[b] University of Chinese Academy of Sciences, Beijing, China
[c] Research School of Earth Sciences, Australian National University, Canberra, Australia

ARTICLE INFO

Keywords:
Australian continent
Lg attenuation model
Geological features
Frequency-dependent Q of Lg waves
Ground motion

ABSTRACT

We estimate the Lg-wave quality factor (Q) across the Australian continent from vertical-component Lg waveforms. A tomographic inversion is performed to construct an Lg attenuation model for 58 frequencies between 0.05 and 10.0 Hz. The available spatial resolution is approximately 1.5° × 1.5° for the 0.5–2.0 Hz band. At 1.0 Hz, the Lg-wave Q over the whole island continent varies from 50 to 1250 with an average value of 850. Significant regional variations in the Lg-wave Q images tie well with many geological features and boundaries in Australia. The cratons in western, northern and southern parts of Australia usually have higher Q values (700–1250), while the volcanic regions, sedimentary basins and orogenic areas in eastern Australia are characterized by increased attenuation (lower Q values, 50–650). We determine the frequency-dependent Q of Lg waves for different blocks across Australia, and find the frequency dependence of Q is much more complex than the traditional single power law representation. When combined with the assumed geometrical spreading relation, the Lg Q maps provide a new way of assessing potential ground motion across the continent for any event location.

1. Introduction

1.1. Lg waves

Lg waves form a prominent component of seismograms for continental sources at regional distances. Lg propagates in continental crust with a group velocity around 3.5 km/s, and was first described by Press and Ewing (1952). Lg is dominated by relatively high frequencies between 0.2 and 5 Hz for continental paths, and usually has an unclear onset but distinct later large amplitudes. A description of the nature of Lg can be made in terms of either the superposition of higher modes of surface waves, or the interference of multiply reflected S waves (e.g., Oliver and Ewing, 1957; Knopoff et al., 1973; Kennett, 1984; Kennett, 1985).

The Lg wave is sensitive to the structure of crust along its propagation path, and so we can hope to extract differences in crustal properties from the nature of the propagation. A detailed discussion of the interaction of Lg waves with structure is provided in Kennett (2002, Chapter 20). Variations in the characteristics of Lg propagation across Asia were recognized by, e.g., Ruzaikan et al., 1977, and similar studies have been made for many parts of the world. Gregersen (1984) showed how the efficiency of Lg-wave propagation (expressed as the relative amplitude of Lg to Sn) could be used to obtain variations in lateral crustal structure heterogeneity. The increasing volumes of high quality data have allowed detailed Lg tomography in many areas (e.g. Zhao et al., 2010).

The Fourier amplitude spectra of Lg waves can be exploited to study crustal attenuation. Typically, tectonically active regions are usually characterized by relatively strong attenuation while stable regions with lower heat flow, thinner sediment cover and a lack of fluids are related to relatively weaker Lg attenuation. Thus, Pasyanos et al. (2009) found higher loss of Lg-wave energy in tectonic regions in the Middle East compared with the shield regions, and Zhao and Xie (2016) found strong attenuation in the continental collision orogenic belt.

The amplitudes of Lg waves are affected by intrinsic attenuation and structural effects, but by building up extensive path coverage we can attempt to isolate the dominant influences in conjunction with information from other fields. For example, Sheehan et al. (2014) suggested that seismic attenuation measurements were able to provide information complementary to seismic velocity estimates and so help to distinguish between compositional and thermal mechanisms for observed anomalies.

1.2. Australian structure

There is a strong contrast in the surface geology of Australia with

* Corresponding author at: Key Laboratory of Earth and Planetary Physics, Institute of Geology and Geophysics, Chinese Academy of Sciences, Beijing, China.
E-mail addresses: weizhi@mail.iggcas.ac.cn (Z. Wei), Brian.Kennett@anu.edu.au (B.L.N. Kennett), zhaolf@mail.iggcas.ac.cn (L.-F. Zhao).

http://dx.doi.org/10.1016/j.tecto.2017.08.022
Received 5 March 2017; Received in revised form 14 August 2017; Accepted 17 August 2017
Available online 18 August 2017
0040-1951/

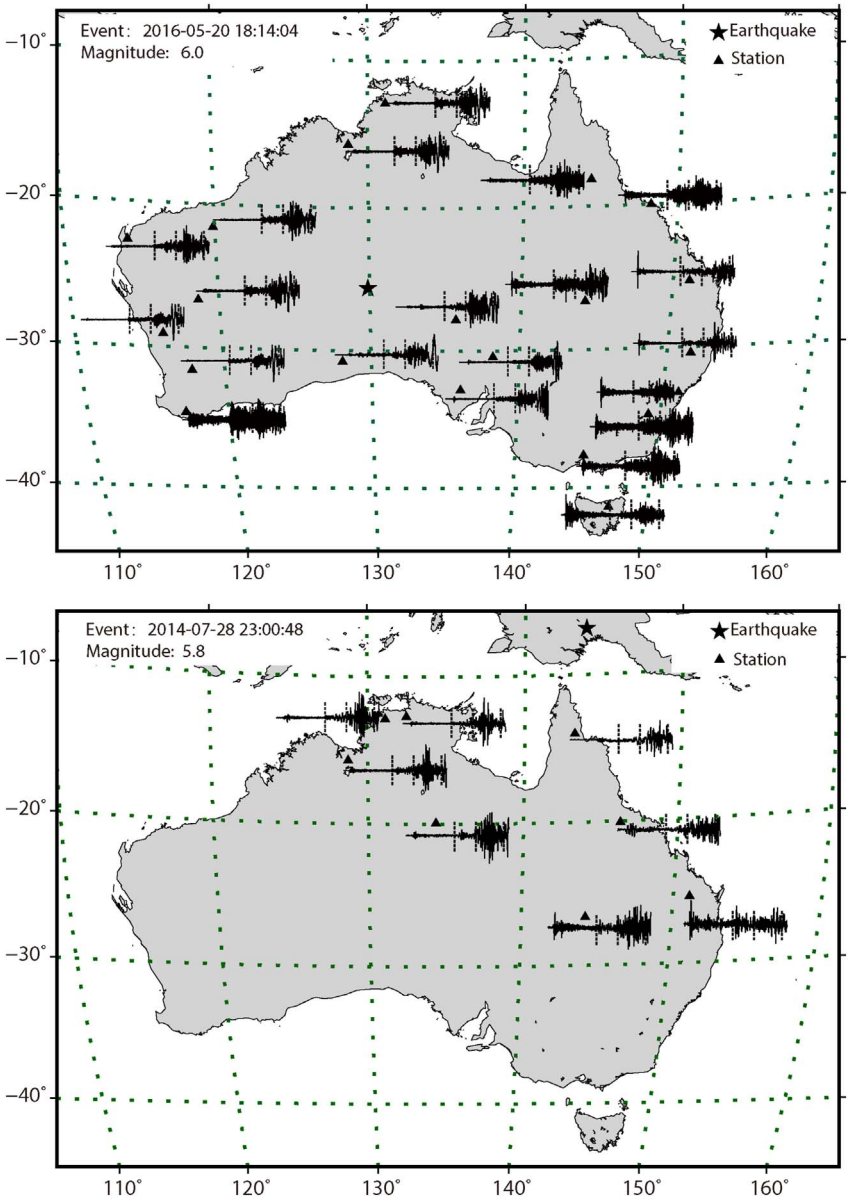

Fig. 1. Selected waveforms for the Mw 6.0 earthquake in Central Australia on 2016 May 20 and the Mb 5.8 earthquake in Papua New Guinea on 2014 July 28. The waveforms are drawn for the velocity window from 8.9 km/s to 2.9 km/s, with dashed line markers at 4.5 km/s (left), 3.7 km/s (middle), and 3.0 km/s (right).

Precambrian rocks in the west and centre which cover two-thirds of the continent, and Phanerozoic fold belts in the east. There has been no mountain building in the ancient continent for more than 200 Myr. The complex development of Australian lithosphere over more than 2 Ga has exerted fundamental influences on the overall tectonic stability and the character of the landscape, the distribution of earthquakes and associated seismic risk, the evolution of sedimentary basins, as well as heat flow and other resource endowment (Kennett and Blewett, 2012).

The structure of the Australian crust has been extensively studied using a wide range of seismological techniques including refraction and reflection, ambient noise, and receiver functions (e.g. Clitheroe et al., 2000; Saygin and Kennett, 2012; Salmon et al., 2013; Korsch and Doublier, 2016). So far, the properties of Lg with their strong sensitivity to crustal variations have not been exploited, and have the potential to provide further understanding of the evolution of the continental lithosphere.

The Tasman Line indicating the transition zone between the Precambrian zone in the west and Phanerozoic region in the east of Australia was originally proposed as the eastern edge of Precambrian outcrop (Hill, 1951). Subsequently, attempts have been made to relate this transition to the break-up of the Rodinian supercontinent (e.g. Scheibner and Veevers, 2000). However, there still exists some uncertainty as to the nature of the transition since there are many conflicting interpretations and models based on different classes of geophysical data (Direen and Crawford, 2003; Kennett et al., 2004). In this work, we try to see if the variations in Lg Q provide further insight into the characteristics of the Tasman line.

For the Australian region, more attention has been paid to seismic attenuation for the entire lithosphere than within the crust. Gudmundsson et al. (1994) provided evidence for a strong change increase in attenuation in the upper mantle beneath the lithosphere in the northern part of the Australian continent. Cheng and Kennett (2002) used a spectral ratio method to estimate the differential attenuation between P and S waves for the paths through the upper-mantle beneath northern Australia. Kennett and Abdullah (2011) extended this work and found that the crust and lithospheric mantle in the eastern part of Australia has larger attenuation compared with that of western and central Australia. The characteristics of the Lg phase provide information on the structure of the Australian continental crust that has not previously been extensively exploited. Bolt (1957) provided a summary of the velocities of Lg waves for the whole Australian continent based on a rather limited set of observations. Bowman and Kennett (1991)

investigated the nature of Lg in the northern part of Central Australia, demonstrating the complex influence of a strong velocity gradient at the base of the crust. Mitchell et al. (1998) mapped out variations in attenuation from a limited suite of Lg coda Q observations and showed a strong contrast between low crustal attenuation in central and western Australia and stronger attenuation in eastern Australia.

Our study covers the whole Australian continent, exploiting the improved seismic data available in the last 10 years in Australia. We employ Lg-wave attenuation tomography over a broad range of frequencies with good ray path coverage and so achieve higher resolution than in previous studies. We also examine the frequency dependency of Q_{Lg} in the main crustal blocks in Australia.

2. Data

We have employed data from the network of permanent stations across the Australian continent, and from temporary broadband deployments made by the Australian National University. Vertical-component seismograms were collected in the period from January 1993 to October 2016, from 469 events recorded at 203 stations with epicentral distances ranging from 2° to 20°. To guarantee suitable signal-to-noise ratios, and avoid influences from complexity in the rupture process of larger earthquakes, we chose seismic events with magnitudes between 3.5 and 6.2. The number of recording stations varies with the size and location of the events. To simultaneously constrain the source function and the regional Q distribution, we require each station to record at least 3 events and each event was to be observed by 3 stations or more. We only use events located on the continent or the continental shelf to ensure that the Lg waves propagate in continental crust, and thereby avoid the complexity of the transitions between oceanic and continental crust (Press and Ewing, 1952; Knopoff et al., 1979; Kennett, 1986; Furumura et al., 2014). There are few earthquakes and seismic stations in most parts of the Northern Territory and Queensland, and so the resolution of structure will be lower in these regions. However, we are able to use many seismic events in New Guinea to improve the ray path coverage into these regions.

Fig. 1 illustrates the waveforms for two of the events used. The first is a Mw 6.0 event in Central Australia in 2016, which was well recorded across the whole continent. The second is an event in New Guinea in 2014 with magnitude Mw 5.8 that gave useful seismograms across northern and eastern Australia, in an area where events are few and stations are widely spaced. The addition of the New Guinea events significantly enhances the available path coverage.

For each seismogram we remove the instrument response, and then employ a group velocity window from 3.7 to 3.0 km/s to isolate the Lg waves. We also extract a segment of noise before the P phase with the same time duration as the Lg wave window. We compute both the Lg-wave and noise spectra for 58 frequency bands distributed log evenly from 0.05 to 10.0 Hz. We calculate the signal-to-noise ratios after removing the influence of the background noise from the Lg waves (Zhao et al., 2010). Only spectral amplitudes with signal-to-noise ratios larger than 2.0 for the individual frequencies are used in the inversions. Fig. 2 illustrates the Fourier spectral amplitudes for Lg waves, for a number of stations after de-noising. We show the raw Lg spectra together with the noise estimate from the segment before the P arrival, as well as the corrected Lg spectra after noise subtraction.

On the whole, the energy loss of Lg waves in propagation across Australia is not severe and high frequency Lg waves can propagate to considerable distances in this ancient continent. This means that we are able to achieve good path coverage with stringent procedures for data quality. Fig. 3 shows the distribution of stations and events used across Australia and its margins as well as into New Guinea.

3. Lg wave Q

We use a procedure to extract Lg wave attenuation across Australia that has previously been used for other areas (e.g., Zhao et al., 2010, 2013b). We assume that the Lg wave propagates along the great circle path between source and station with geometrical spreading proportional to the square root of epicentral distance. This spreading function is suitable for a crust with a sharp transition to the mantle, but may not give as effective a representation where the transition from crust to mantle is gradational as in parts of the Northern Territory (Bowman and Kennett, 1991). The Lg amplitude $A(f, \Delta)$ for a station at epicentral distance Δ and frequency f is represented as.

$$A(f,\Delta) \propto \Delta^{-1/2} \exp\{-\pi f \int_{ray} \mathrm{ds}\, Q^{-1}(\mathbf{x},f) \Big/ V\} \quad (1)$$

where V is the group velocity for the Lg pulse and $Q^{-1}(\mathbf{x}, f)$ describes the local attenuation of Lg as a function of position $\mathbf{x}$. The total attenuation is calculated as an integral along the ray path between source and station. When we invert for Lg Q, any deviations from the assumed geometrical spreading will be mapped into an apparent Q; thus.

$$Q^{-1}{}_{\mathrm{est}} = Q^{-1}{}_{\mathrm{int}} + Q^{-1}{}_{\mathrm{str}} \quad (2)$$

where Q_{int} arises from intrinsic attenuation, and Q_{str} from any structural effects, including deviations from the assumed geometrical spreading. When Q values are high, structural influences are weak, but in any regions with low Q (high attenuation) we need to be aware of a possible contribution from variations in structure.

We consider Q as a function of location and frequency, and simultaneously invert for the Lg-wave Q distribution across the Australian continent for frequency bands distributed log evenly between 0.05 and 10.0 Hz. We concentrate on the passage of the Lg waves, whilst recognising that there will be source and site response issues that are hard to resolve from individual spectra. We rely on the broad ensemble of path observations, and treat such effects as contributions to measurement error.

We build an initial Q model by using two-station techniques. When two stations record the same earthquake approximately on the same great-circle, Q for the path between the stations based on a specific Lg spreading function (Yang, 2002) can be extracted by calculating the spectral ratio (Zhao et al., 2013a). The average of the path specific Q values provides a uniform starting model for the inversion of the laterally varying Lg Q model. In the Supplementary Material Section S.1 we illustrate the distribution of paths used for the two-station analysis for the 1 Hz band, along with the full ray path set.

For the tomographic inversion, the model is based on a uniform grid across the continent. We choose the spatial resolution for each frequency based on experiments with the available path coverage. We use the actual geometry of the sources and receivers to test how well the artificial Lg-wave Q anomalies can be recovered with our inversion procedure. Resolution tests were conducted independently for the various frequencies using a checker-board approach with variable grid sizes from 0.9° × 0.9° to 2.5° × 2.5° with step of 0.1°. For each frequency, ± 7% checker-shaped perturbations are added to a constant background Q model that is used to generate a theoretical spectral dataset. To simulate the noise in real data, we also added 5% rms random noise to the spectral data. We evaluate the quality of the inversion by the degree of the recovery of the original checker-board patterns from the synthetic data. Because the signal-to-noise ratios vary between frequencies, the available data points are different and there is some difference in resolution at different frequencies. Examples of the influence of different grid sizes are presented in the Supplementary Material - Section S.2.

For the tomographic inversion, we use an iterative approach with sequential linearisation of the tomographic equations. At each step, we compute the L_2 residuals between the observed and theoretical amplitude spectra of the Lg waves. The suite of linearised tomographic equations is solved using the LSQR algorithm (Paige and Saunders, 1982). We start with equal weighting to data fit and damping to the initial Q model. The damping is progressively reduced as the iterations

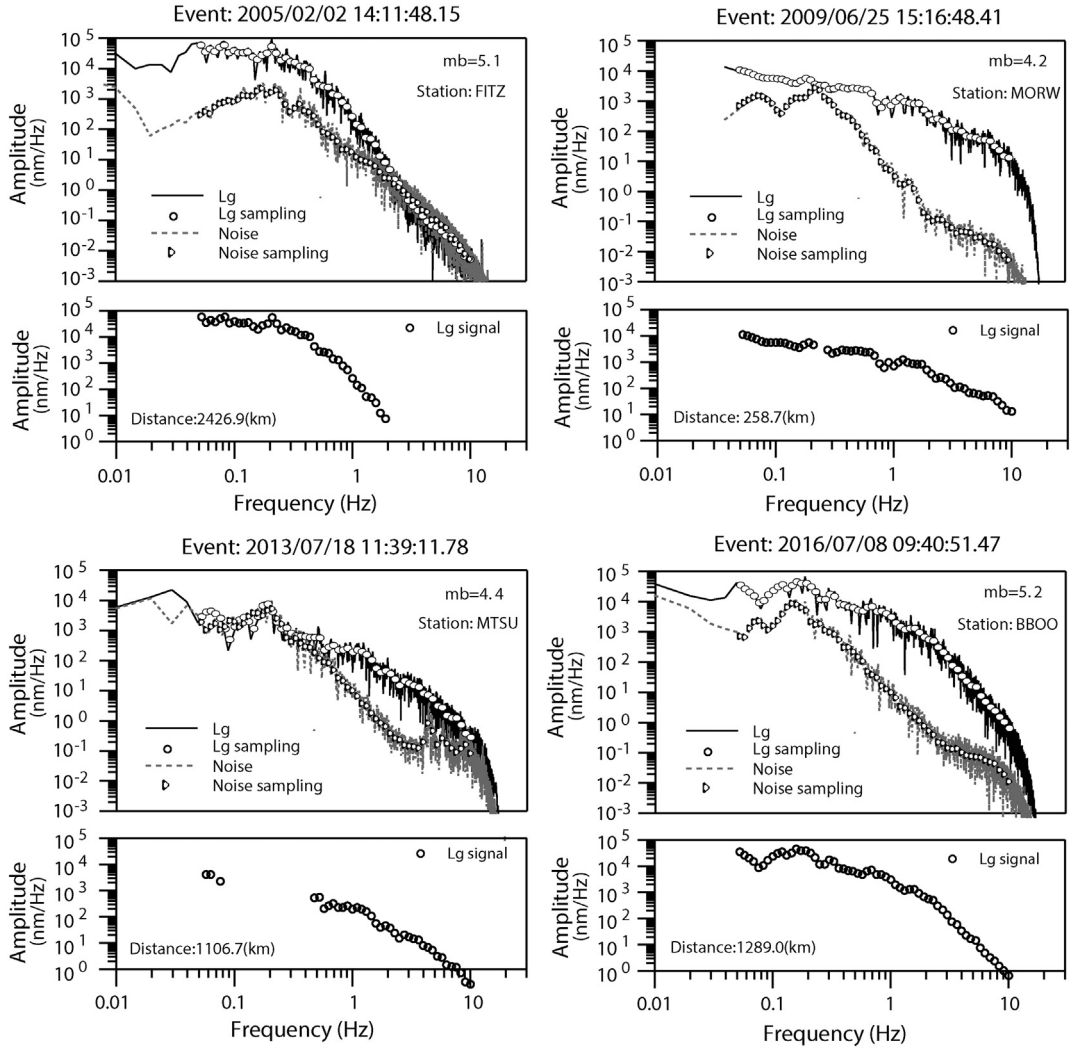

Fig. 2. Images of the Fourier spectral amplitudes for Lg waves and the background noise as a function of frequency. In the lower panel for each station the spectral amplitudes are shown after noise removal.

proceed: for the *k*th iteration the weight of the damping term is given by.

$$\lambda_k = \alpha^{(k-1)} \tag{3}$$

where the coefficient α is taken as 0.7. We employ 150 iterations for the inversion at each frequency, and then select the model with the smallest total residual.

In addition to the tomographic inversion we examine the frequency dependence of Lg Q across the continent. For each geological block, we calculate the average Q value for each frequency and use a power-law relationship of the form $Q_0 f^{\eta}$ between Lg Q and frequency, with least square minimization to estimate the exponent η.

4. Lg attenuation in Australia

The inversion domain for Lg-wave attenuation covers the entire Australian continent with a longitude span of 40° and a latitude span of 35°. Lg-wave Q models have been constructed for a suite of 58 frequencies between 0.05 and 10.0 Hz. We focus on the attenuation measurements for frequencies above 0.5 Hz, due to the larger noise levels for lower frequencies. We endeavour to characterize the differences in Lg attenuation and velocities between regions and the spatial variation in the frequency dependence of Q.

For each frequency, we undertake 150 iterations of the tomographic inversion, and then adopt the Q model that has the smallest residual error. For the frequency bands centered at 0.5 Hz, 1.0 Hz and 2.1 Hz we display in Fig. 4 the Lg Q models, the ray path coverage and the corresponding resolution tests. Our selection criteria mean that the number of suitable ray-paths differs slightly between frequency bands, and so the potential resolution for Lg Q maps is frequency dependent. In the regions with the best sampling, features with a size around 1.0° × 1.0° can be resolved, but generally a slightly larger grid size gives the best results. Thus we use grids with a spacing of 1.5° × 1.5° from 0.5 Hz to 2.1 Hz. With the relatively high density of ray-path coverage across the whole continent, the recovery of structure is good in most parts of Australia. Although parts of the margins of the continent have more limited ray sampling, the checker-board tests still show reasonable results (see also Supplementary Material Section S.2).

4.1. Spatial variation of Q across Australia

We display the absolute Lg Q values with the same colour scale in all maps in Fig. 4 with a Q range from 50 to 1250. This means the Lg Q variations can be easily compared between images. Most parts of Australia are characterized by relatively low Lg-wave attenuation (high Q). The North Australian Craton, West Australian Craton and most parts of South Australian Craton, and parts of the Lachlan Orogen and New England Orogen are characterized by distinctly lower attenuation than the average, particularly the southern part of the West Australian

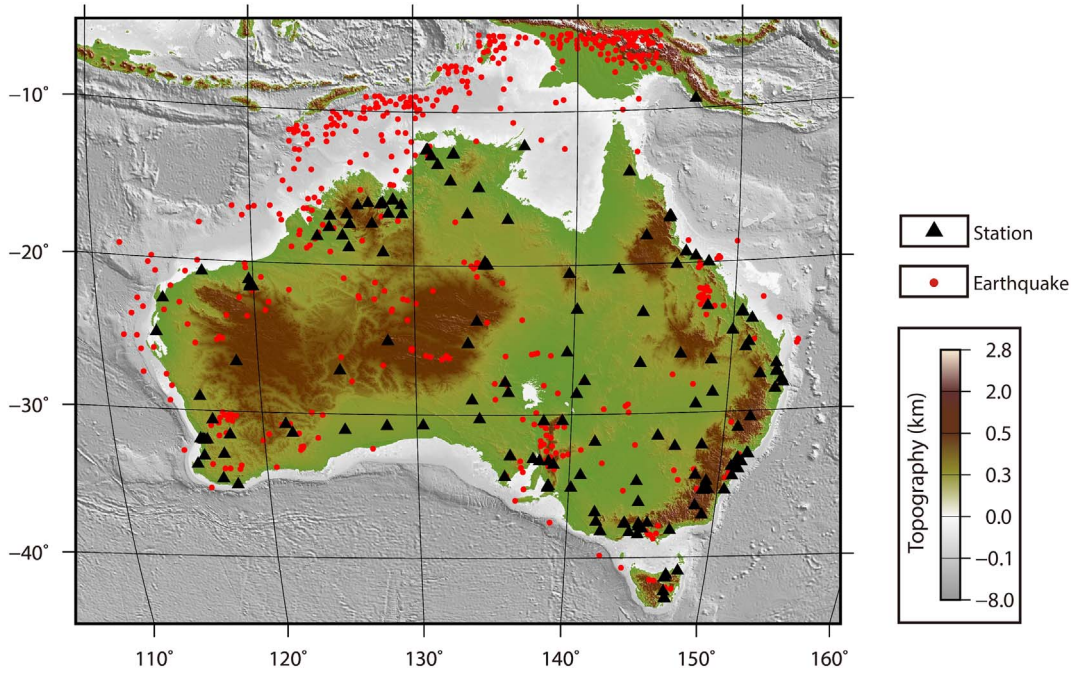

Fig. 3. The distribution of the stations and events employed in the Lg Q study superimposed on the topography of the Australian region. Stations are indicated by black triangles and events by red filled circles. (For interpretation of the references to colour in this figure legend, the reader is referred to the web version of this article.)

Craton the Yilgarn Craton where Q exceeds 1100. Parts of northwestern Australia, western central Australia and some regions of eastern Australia display higher attenuation (with lower Q). There are some regions with rather high Lg-wave attenuation, e.g., parts of Tasman Fold Belt in eastern Australia where apparent Lg Q values are below 100. In Fig. 5, we provide an average Lg Q map for the frequency band between 0.5 and 2.1 Hz to provide an overall impression of the Lg-wave attenuation distribution across the Australian continent. This map is calculated by averaging the values of Lg Q for each grid point from the values for the frequency bands distributed log evenly in the interval 0.5 to 2.1 Hz.

The spatial variation of the Lg Q for Australia, for the 0.6–2.0 frequency band, is illustrated in Fig. 6 for profiles at constant latitude from 20°S to 32°S with a 4° step. In Fig. 6 we provide an indication of the likely uncertainty in Lg Q as a grey band about profile. This uncertainty estimate is based on both the variability in the path estimates for Q, and consistency between inversions with different parameterisations. The Lg Q model along 20°S may be divided into three segments with distinctly different features. In the west across the Canning Basin to just west of the Arunta Block, the model displays quite low and varying Q values between 50 and 600. Through the central segment across the North Australian Craton, the Q is high and nearly constant. From the east of the Northern Territory to the easternmost segment, Q decreases steeply toward east, from about 1000 at the edge of North Australian Craton to below 100 at 155°E. The Lg Q variations are generally more subdued on the other profiles, but display a significant contrast between the Pinjara Orogen ($Q \sim 300$) on the western margin of the continent and the West Australian Craton with $Q > 900$.

The multi-frequency analysis of the behaviour of Lg Q enables us to examine the nature of the frequency dependence without imposing an a priori model. We illustrate the frequency behaviour for a number of geological blocks in Fig. 7, and summarise the frequency characteristics for the major geological provinces in Table 1. From the log-log plots shown in Fig. 7 we find that the relationship between frequency and Lg Q in Australia is not simply a power law. For the continent as a whole there is a distinct difference between the frequency dependence below around 1.0 Hz and above. We find that it is reasonable to fit the Q behaviour over three frequency bands (0.05–0.5 Hz, 0.6–1.0 Hz, 1.1–4.0 Hz), and estimate the geographic distribution of η for each band. We need to employ rather larger cell sizes (5° × 5°) than for Q itself, but nevertheless a clear pattern of variation can be seen in Fig. 8. For the low-frequency band (0.05–0.5 Hz) the value of η is generally above 0.7, though lower exponents are seen in the northeast and southeast, with a comparable band also extending south from the Canning Basin. For the 0.6–1.0 Hz band the frequency dependence is generally weak but there are notable contrasts between the Yilgarn Craton and its surroundings. A strong frequency exponent is only seen for narrow zones along the continental margins, where resolution is limited. In the highest frequency band (1.1–4.0 Hz), the strongest frequency dependence occurs in the Kimberley block and the northern part of the North Australian Craton.

Much of Australia is covered in a thin regolith veneer obscuring the solid geology. Most sedimentary basins have thicknesses much less than 7 km. The few basins with thick sedimentary deposits, such as Canning Basin, Amadeus Basin and Eromanga Basin, are well imaged with strong loss energy of Lg waves especially at higher frequencies. At 2.0 Hz we can note the bifurcation of lowered Q values around the Musgrave Block, reflecting the presence of thickened sediments. Even where sediments lie on cratonic crust, as for example in the North Australia craton, their influence is weak and Lg Q values remain well above the average Q value of 850.

The strongest large-scale contrast in crustal structure in Australia occurs near 137°E between 24° and 29°S, where the crust thins rapidly from more than 50 km thick to less than 30 km thick. It is likely that energy loss into the mantle for Lg waves crossing this transition (cf. Kennett, 1986) contributes to the lowered Q evident in the Q image at 0.5 Hz (Fig. 4). A similar contrast to thickened crust at the south of the Mt. Isa block may also contribute to the east-west transition from relatively high to moderate Q at 23°S.

Although a gradient zone at the base of the crust also modifies Lg propagation characteristics (Bowman and Kennett, 1991) we do not see much influence in the North Australian craton, where such gradients are common. But, such effects may help to account for the higher attenuation in parts of the Proterozoic in Central Australia and the Palaeozoic Lachlan fold belt in southeastern Australia with thick crust.

In the Supplementary material (Section S.4) we present cross-sections of Lg Q as a function of frequency for slices at constant latitude

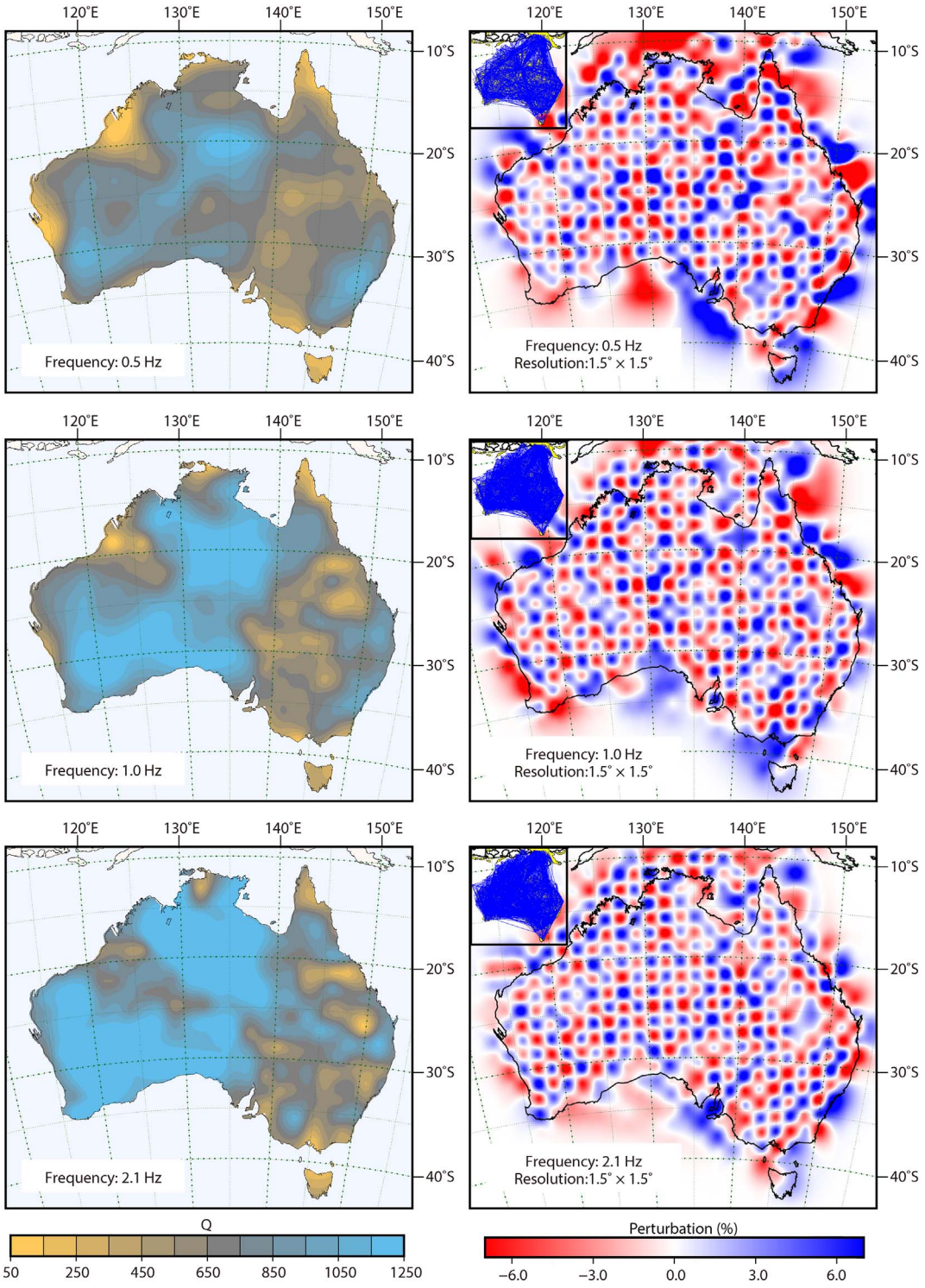

Fig. 4. Lg Q models, the ray path coverage and resolution tests for the frequency bands centered at 0.5 Hz, 1.0 Hz and 2.1 Hz.

and longitude. Although some features in the frequency patters can be related to changes in crustal thickness, structural effects do not dominate the patterns.

4.2. Comparison of Australian Lg Q with other continents

In Table 2 we present a comparison of the estimate of Lg Q for the shield area of Australia with results from other stable continents at 1 Hz. These regions are among the most stable areas on Earth, with relatively low attenuation. For instance, the average Lg Q value for the Indian shield, which occupies two-thirds of the southern Indian peninsula, is lower than 600; the Canadian Shield, which is mainly covered by Precambrian rocks, is characterized by low Lg-wave attenuation (Q = 900). Both southern and northern Africa have Lg Q values lower than 650, similar to the central and northeast United States. The Lg attenuation in the Australian continent is weak, and the average Lg Q (850) of the continent is larger than for most stable regions.

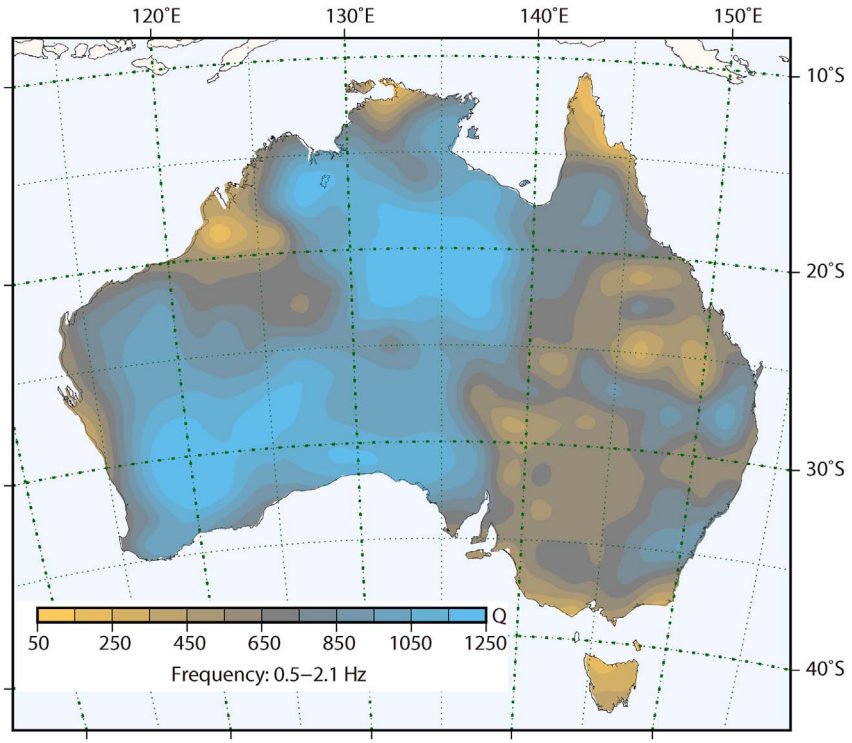

Fig. 5. Map of average Lg Q over the frequency band from 0.5 to 2.1 Hz.

5. Discussion

In Fig. 9 we bring together the full range of information on Lg behaviour for Australia, linked to the main tectonic provinces. We display the average Lg Q in the frequency band 0.6–1.0 Hz in Fig. 9(a), and alongside this we show the frequency exponent η for the same frequency band (Fig. 9b). For this frequency-band Lg waves should sample the entire crust with some modest emphasis on the shallower regions. The third panel (Fig. 9c) displays the group velocity for Lg waves (see Supplementary Material S.3) that shows a good general correlation with the pattern of Lg Q. The last panel of Fig. 9 shows the main tectonic units across Australia, with their ages indicated, as well as the location of the Tasman Line (from Direen and Crawford, 2003). Each of the various aspects of Lg propagation has a strong correlation with the patterns of geological provinces across Australia, but in different ways.

As we can see from Figs. 5 and 9a, much of the Australian continent

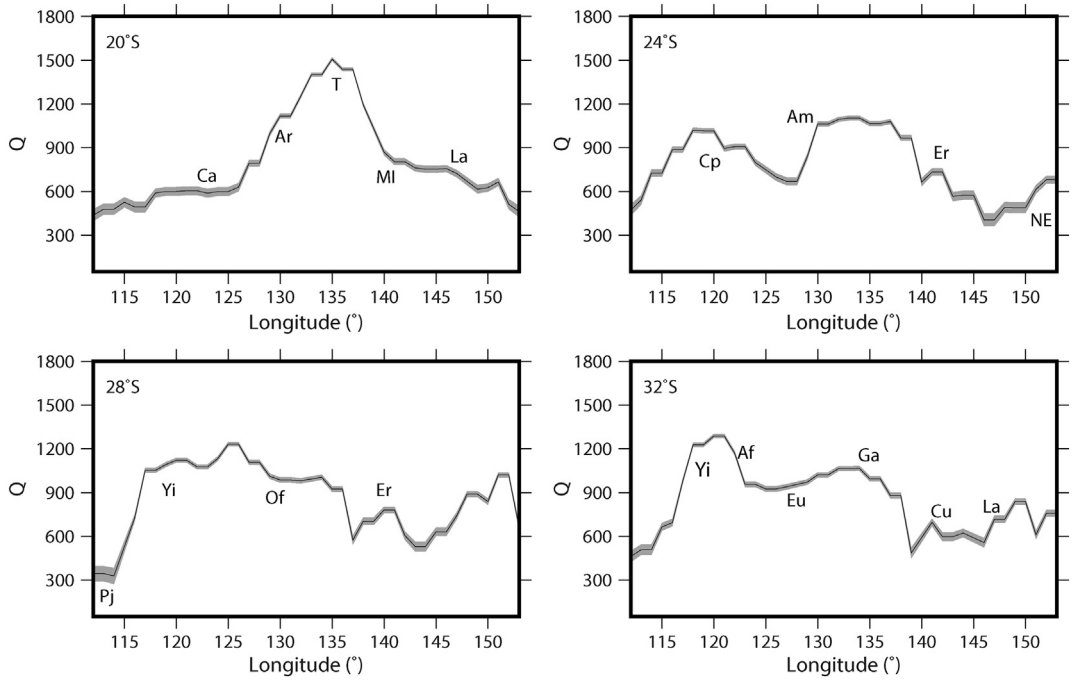

Fig. 6. Lg Q values for profiles at constant latitude across Australia from 20°S to 32°S with a step of 4° in latitude. The uncertainties in the Q values along the profiles are indicated by the grey band. Geological provinces are annotated (as in Fig. 9d). Key to marked features: Af - Albany-Fraser belt, Ar - Arunta Block, Am - Amadeus Basin, Ca - Canning basin, Cp - Capricorn Orogen, Cu - Curnamona Craton, Er - Eromanga basin, Eu - Eucla basin, Ga - Gawler craton, La - Lachlan Orogen, MI - Mt. Isa block, NE - New England Orogen, Of - Officer basin, Pj - Pinjarra Orogen, T - Tennant Creek block, Yi - Yilgarn craton.

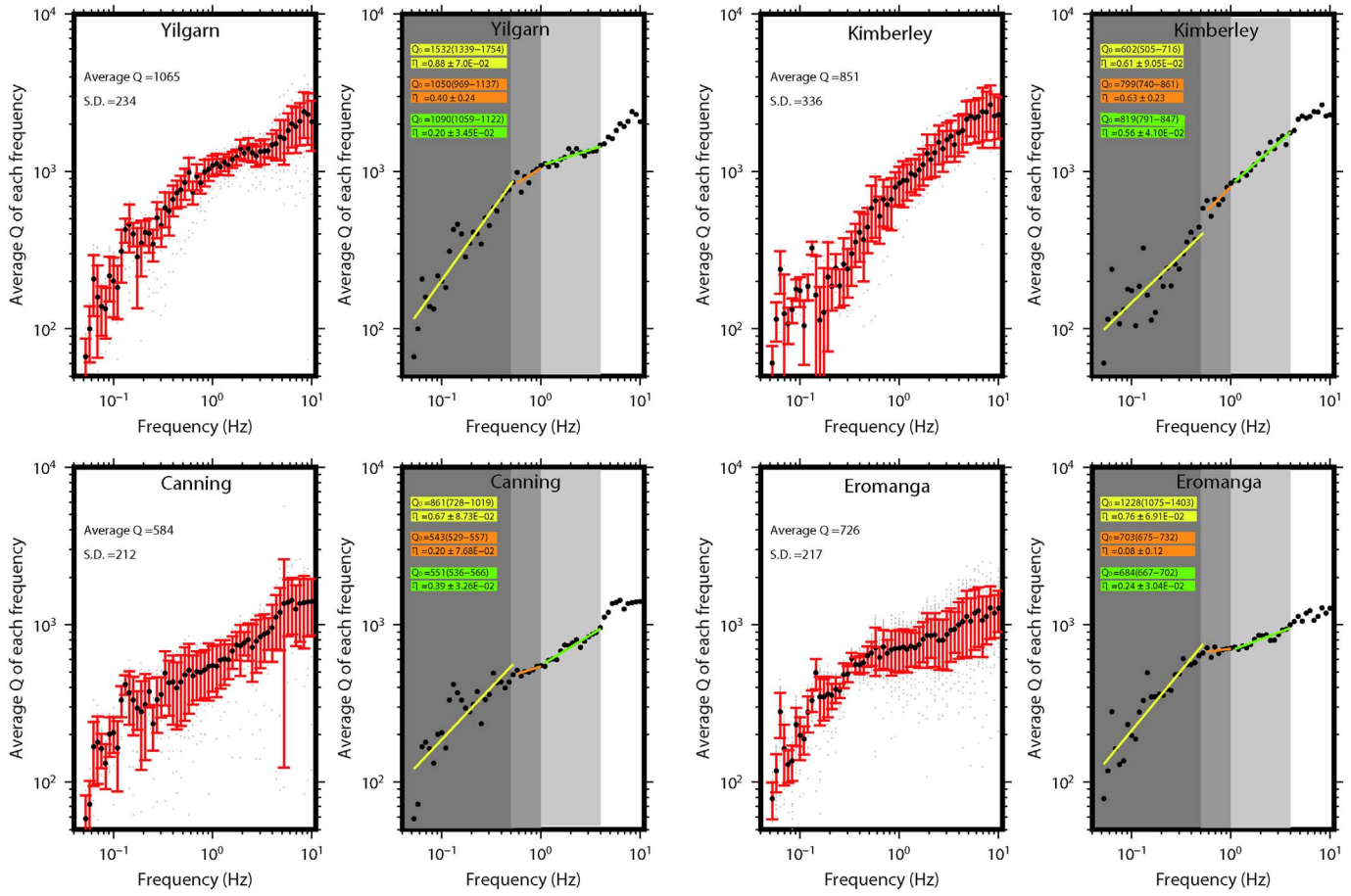

Fig. 7. Examples of the frequency dependences of Lg Q, and the average Q values for different geological blocks.

has relatively high Lg Q values, though there are regions with quite low Q. The Q values for most Proterozoic and Paleozoic regions in Australia, such as the Amadeus Basin and Georgetown inlier, are comparable to the Lg Q of the Canadian Shield, which is 900 at 1 Hz (Hasegawa, 1985), the central United States with Q values larger than 1052 above 1.5 Hz (Benz et al., 1997), the stable part of South America whose Q values range between 550 and 1000 (De Souza and Mitchell, 1998) as well as stable portions of Eurasia with values larger than 600. The Archean Yilgarn craton has very high Q values, though the average Q is a little lower in the Archean Pilbara craton with thinner crust (around 30 km thick). There is a tendency for the Q to increase with the age of the crust.

5.1. Lg Q patterns

The tomographic images of Lg attenuation structure indicate a good

Table 1
Frequency dependence of Lg Q and the average Q values of 0.5–2.1 Hz for major geological provinces in Australia (as displayed in Fig. 9d).

Geological block	Average Q (0.5–2.1 Hz)	Q_0 (0.05–0.5 Hz)	η (0.05–0.5 Hz)	Q_0 (0.6–1.0 Hz)	η (0.6–1.0 Hz)	Q_0 (1.1–4.0 Hz)	η (1.1–4.0 Hz)
AF	915 ± 211	1108 (916–1341)	0.84 ± 0.10	907 (854–962)	0.55 ± 0.18	973 (933–1014)	0.20 ± 0.05
Ar	1074 ± 174	1737 (1521–1984)	0.86 ± 0.07	1064 (986–1147)	0.099 ± 0.23	989 (964–1015)	0.28 ± 0.03
Am	882 ± 130	1488 (1274–1739)	0.84 ± 0.08	970 (909–1036)	0.23 ± 0.20	835 (761–916)	0.015 ± 0.11
Eu	1066 ± 167	1307 (1080–1582)	0.80 ± 0.10	1102 (1038–1170)	0.42 ± 0.18	1134 (1099–1171)	0.12 ± 0.04
Ga	1007 ± 176	1145 (966–1357)	0.68 ± 0.09	1055 (984–1132)	0.21 ± 0.21	1055(1022–1089)	−0.02 ± 0.04
Ge	844 ± 122	1067 (928–1227)	0.65 ± 0.07	914 (849–983)	0.60 ± 0.22	880 (836–926)	0.08 ± 0.06
Ha	878 ± 192	1373 (1197–1576)	0.89 ± 0.07	819 (749–895)	0.32 ± 0.27	821 (791–852)	0.46 ± 0.04
La	769 ± 170	1459 (1284–1658)	0.74 ± 0.07	750 (689–806)	−0.28 ± 0.22	721 (704–738)	−0.02 ± 0.03
Mc	954 ± 176	1210 (1042–1406)	0.88 ± 0.08	998 (916–1088)	0.45 ± 0.26	962 (915–1012)	0.16 ± 0.06
MI	849 ± 111	1253 (1022–1538)	0.81 ± 0.11	993 (942–1047)	0.40 ± 0.16	835 (774–901)	−0.043 ± 0.09
Mu	997 ± 139	1382 (1168–1635)	0.82 ± 0.09	1037 (972–1107)	0.38 ± 0.20	978 (950–1008)	0.24 ± 0.04
NE	725 ± 148	874 (767–995)	0.69 ± 0.07	764 (727–802)	0.54 ± 0.15	785 (750–821)	0.014 ± 0.05
Of	1045 ± 167	1233 (1050–1448)	0.71 ± 0.08	1086 (1020–1156)	0.38 ± 0.20	1041 (1020–1062)	0.20 ± 0.02
Pi	902 ± 146	1414 (1212–1650)	0.87 ± 0.08	843 (781–911)	0.16 ± 0.23	932 (875–993)	0.087 ± 0.08
T	1326 ± 232	1805 (1523–2139)	0.84 ± 0.09	1256 (1143–1380)	0.15 ± 0.28	1088 (1040–1139)	0.70 ± 0.05
Yi	1065 ± 234	1532 (1339–1754)	0.88 ± 0.07	1050 (969–1137)	0.40 ± 0.24	1090 (1059–1122)	0.20 ± 0.03
Ki	851 ± 336	602 (505–716)	0.61 ± 0.09	799 (740–861)	0.63 ± 0.23	819 (791–847)	0.56 ± 0.04
Ca	584 ± 212	861 (728–1019)	0.67 ± 0.09	543 (529–557)	0.20 ± 0.08	551 (536–566)	0.39 ± 0.03
Er	726 ± 217	1228 (1075–1403)	0.76 ± 0.07	703 (675–732)	0.08 ± 0.12	684 (667–702)	0.24 ± 0.03

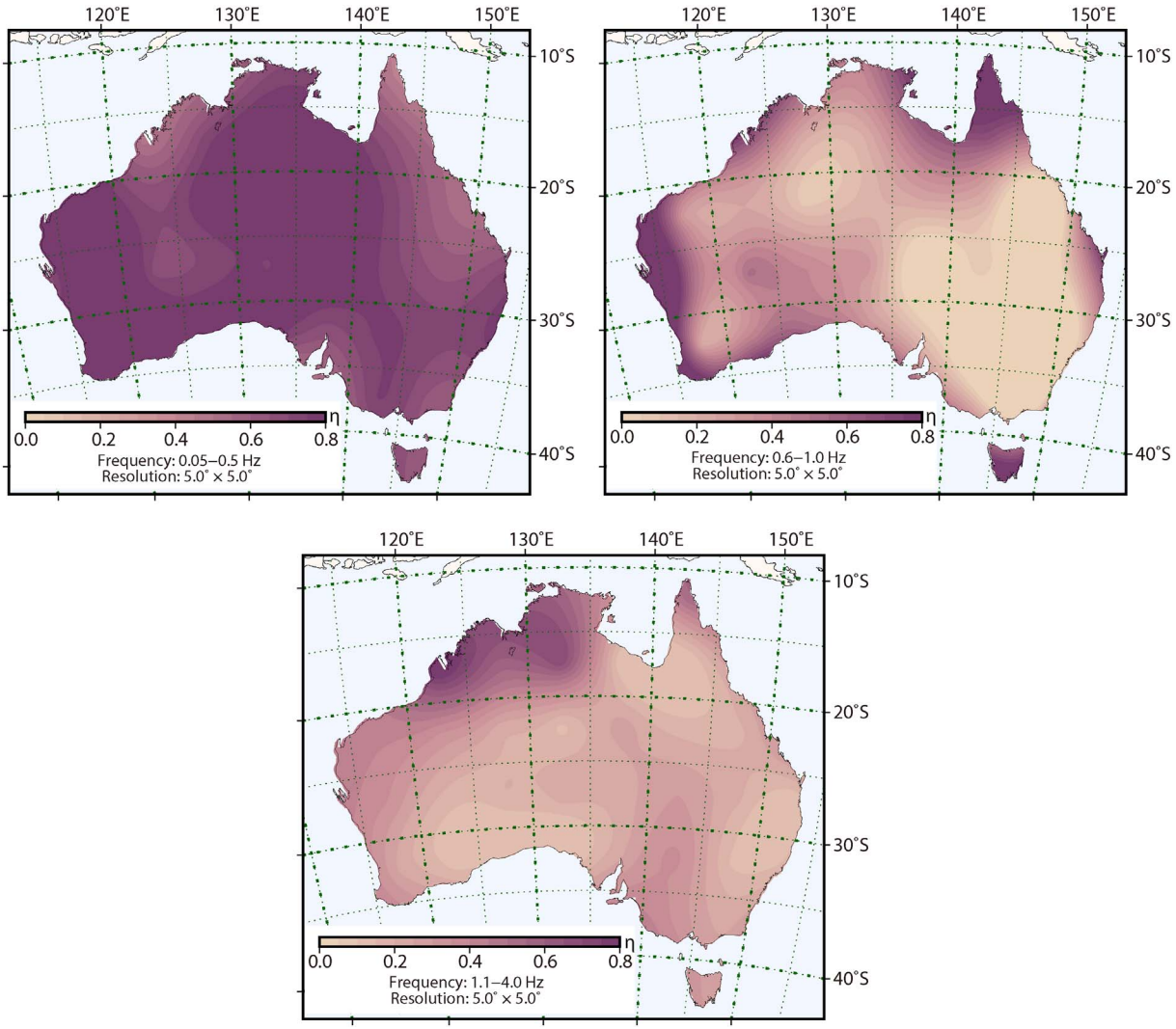

Fig. 8. The geographic distribution of the frequency exponent η for the frequency bands centered at 0.5 Hz, 1.0 Hz and 2.1 Hz.

Table 2
Reported Lg Q or Lg coda Q for some stable continents.

Regions	Q (1 Hz)	Sources
Australian shield	1050	Our study
North China craton	374	Zhao et al. (2013a)
Indian shield	< 600	Singh et al. (2011)
Northeast United States	650	Erickson et al. (2004)
Central United States	640	Erickson et al. (2004)
Northern Africa	650	Issak and Camerlynck (2016)
Southern Africa	600	Chow et al. (1980)
Canadian shield	900	Hasegawa (1985)
Southeastern Canada	670	Atkinson and Mereu (1992)
Siberian craton	< 900	Mitchell et al. (1997)
East European shield	< 500	Mitchell et al. (1997)
Arabian shield	< 500	Mitchell et al. (1997)

tie between the patterns of variation in Lg-wave Q and the main tectonic features of the Australian continent, and the average Lg Q values increase with increasing frequency. However, at all frequencies, there is a distinctive anomaly with relatively high attenuation (low Q) in the Tasman Fold Belt compared with the regions in central and western Australia.

The Archean Pilbara and Yilgarn cratons that cover much of Western Australia show rather low Lg-wave attenuation. The Capricorn Orogen between these two cratons shows only slightly lower Lg Q, while the Canning Basin to the east has relatively high attenuation. In the northwest of the Canning Basin there are thick sediments in the Fitzroy trough with apparent Lg Q values below 150. At the eastern margin of the Yilgarn craton, the apparent increase in Lg-wave attenuation may well be influenced by rather thick crust beneath the Musgrave block, with a gradational base to the crust rather than a sharp Moho. In the Northern Territory, the Kimberley block, Georgetown Inlier and Arunta Block have distinctive low Lg-wave attenuation (high Q). The North Australian craton is also generally characterized by low Lg-wave attenuation. In central Australia, the crust still has patches of high Lg Q, but the values are somewhat lower than in the West Australian craton, especially for the Amadeus Basin and Musgrave Block. Much of the South Australian craton displays low Lg attenuation, though the Curnamona craton shows only moderate Q (~600). The Eucla Basin shows reduced Q at lower frequencies, but is comparable to the cratons at 2.1 Hz.

Large portions of eastern Australia are dominated by moderate Lg-wave attenuation, though areas with thinner crust tend to show lower Q. The Lachlan Fold Belt and New England Orogen have relatively high Q (> 800), similar to the cratons in western Australia. Tasmania is not adequately resolved with the available data.

Lg-wave attenuation is sensitive to the presence of areas with locally higher temperature. The regions where geothermal effects are well recognized, such as the corner between Queensland and South Australia in the Eromanga basin show extremely strong Lg-wave attenuation

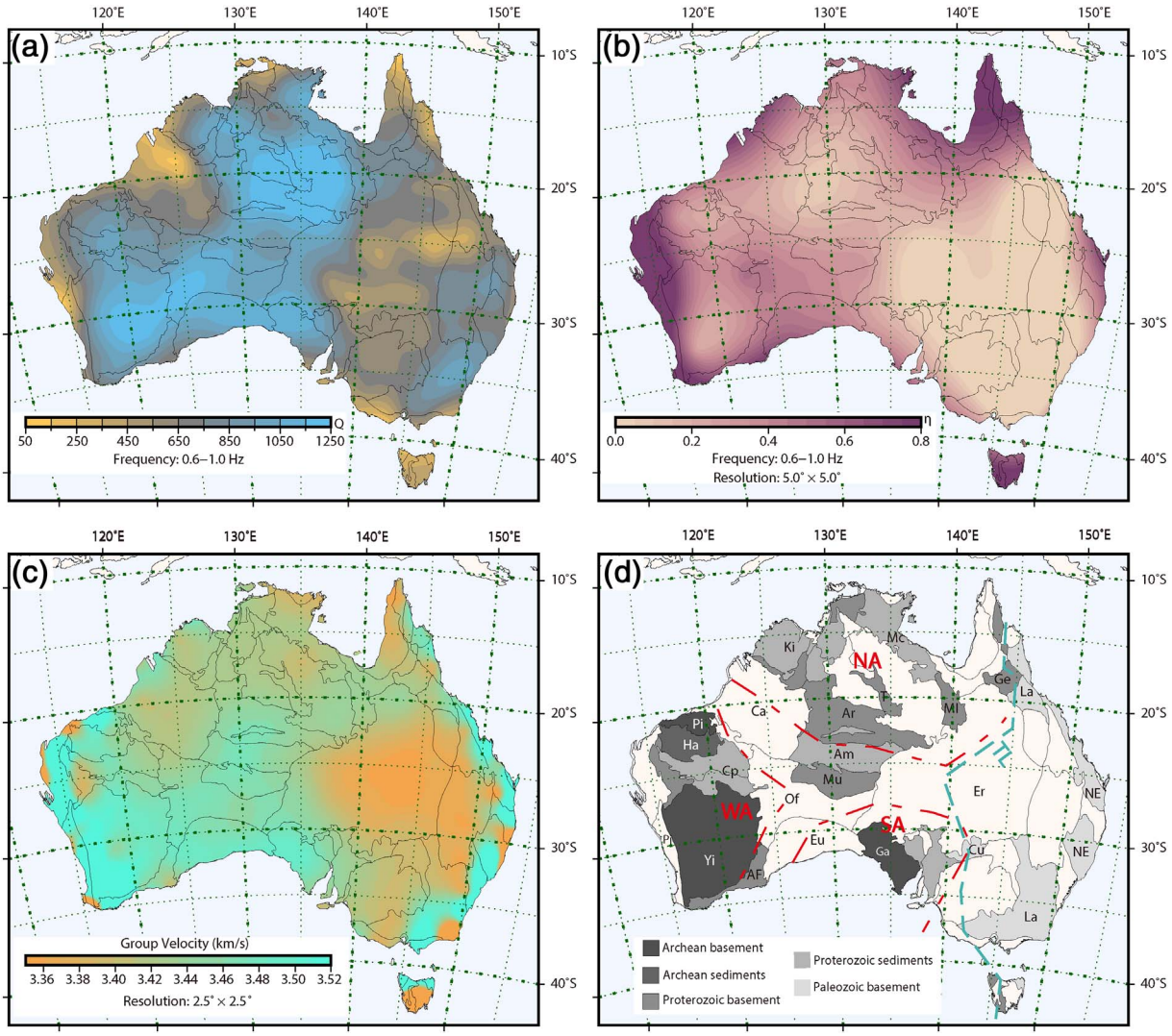

Fig. 9. Comparison between maps of (a) average Lg Q, (b) frequency exponent η, (c) Lg-wave group velocity, and (d) Australian crustal elements and craton boundaries (in red). The approximate location of the Tasman line (after Direen and Crawford, 2003) is indicated by a dashed line in cyan.
Key to marked features: AF - Albany-Fraser belt, Ar - Arunta Block, Am - Amadeus Basin, Ca - Canning basin, Cp - Capricorn Orogen, Cu - Curnomona Craton, Er - Eromanga basin, Eu - Eucla basin, Ga - Gawler craton, Ge - Georgetown inlier, Ha - Hammersley Basin, Ki - Kimberley block, La - Lachlan Orogen, Mc - MacArthur basin, MI - Mt. Isa block, Mu - Musgrave block, NE - New England Orogen, Of - Officer basin, Pi - Pilbara craton, Pj - Pinjarra Orogen, T - Tennant Creek block, Yi - Yilgarn craton. NA – North Australian craton, WA – West Australian craton, SA- South Australian craton, TL – Tasman Line. (For interpretation of the references to colour in this figure legend, the reader is referred to the web version of this article.)

whose Q values are even less than 200. Variations in temperature are expected to play a large part in controlling attenuation behaviour, with a decrease in temperature leading to increased Q values. Some regions with higher seismic wavespeed, such as the Amadeus Basin, are well marked by localized high attenuation, most likely because seismic attenuation has a stronger sensitivity to temperature than seismic wavespeed (e.g., Kennett and Abdullah, 2011; Zhao and Xie, 2016). The relation between seismic wave attenuation and temperature is highly nonlinear (e.g., Jackson and Faul, 2010), especially as the solidus is approached. However, seismic wavespeeds do not always decrease with increase of temperature. Sometimes the increase in velocity caused by increasing pressure can dominate the decrease of velocity due to increasing temperature in the crust (Khazanehdari et al., 2000).

Using stacked correlations of ambient noise between station pairs, Saygin and Kennett (2012) found the group velocity maps of Rayleigh waves and Love waves in Australia have strong correlation with sediment thickness at short periods, and the zones with fast velocity associated with the ancient cratonic regions. However, there is no clear expression of the Tasman Line in these velocity maps. In the crust beneath eastern Australia, the lower seismic wavespeeds are correlated with an increase in seismic attenuation and abrupt changes from high shear wavespeed to low wavespeed are also marked by sharp change from high to low Q. A similar correlation also exists in other regions, such as Canning Basin in the western part of Australia, where low seismic S wavespeed is well correlated with significantly decreased Q.

Clitheroe et al. (2000) reported that parts of the transition from the thick crust beneath central Australia to the thinner crust beneath eastern Australia are in good agreement with the Tasman line, but this correlation has become less clear as much more information on the depth to Moho has been accumulated (Kennett et al., 2011; Salmon et al., 2013). We note that, particularly in the Lg Q image at 1 Hz, there is a clear boundary that has high correlation with the expected location of Tasman Line between the Precambrian zone and Phanerozoic zone. The crust beneath and around the Tasman Line has lower values of Q (between 50 and 700). High temperature anomalies, fluid effects during Devonian and Carboniferous orogenisis and the sedimentation in Jurassic and Triassic times are likely to contribute to the strong attenuation in these regions (Mitchell et al., 1998). Further the strong sensitivity of

Lg waves to structural contrasts means that we expect variations in Lg amplitude (and hence apparent Q) associated with rapid transitions in crustal thickness. In particular the lowered Lg Q in the southern part of Central Australia is likely to be enhanced by the zones of sharp contrast in depth to Moho that have a strong impact on the gravity field.

5.2. Frequency dependence of Lg Q

The frequency dependence of Lg Q across the continent is quite complex. With increasing frequency we expect the Lg amplitudes to be more sensitive to shallower structure, and as a result the differences between the patterns at different frequencies will include a component associated with differential sampling of the crust. It is likely that the varying sampling also contributes to deviations from any simple Q power law with frequency. For frequencies below 0.5 Hz the signal to noise ratio is rather low so the variance of the frequency dependence results is large. The most consistent values come in the band around 2 Hz. The variations at higher frequencies may well come from near-surface variations, and those at the lower frequencies are likely to include components dependent on the nature of the lower crust. There is no single simple descriptor for the frequency dependence of Q across the Australian continent, which is not surprising given its long and complex tectonic history.

The average Lg Q distribution shows a distinct narrow stripe of lower Q in the Pinjarra Orogen along the western coast of Australia, but this is too small to be fully resolved in the other images, though there is tendency to more rapid frequency variation in this area. The Canning basin also stands out as a zone of lowered Q, with somewhat less frequency dependence and mildly reduced Lg group velocity. In the frequency dependence plot, the Kimberly block has a notable difference from its surroundings with rapid frequency variation of Q, but this is not reflected in the other fields. Similarly the eastern part of the North Australian Craton shows strong frequency variation of Q with a sharp boundary to the south of Mt. Isa. The area to the south of this boundary, with low frequency variation of Q, also largely corresponds to a zone of rather low Lg group velocity. The eastern boundary in Q itself is closer to 140°E and the regions of lowered Q are more localized, mostly likely reflecting temperature variations at depth beneath the sedimentary basins.

The Albany-Fraser Belt, Eucla and southern Officer Basin separating the West and South Australian cratons have more frequency variation in Q than the cratons, indicating a change in crustal character. A further prominent feature in the frequency variation of Q between 0.6 and 1.0 Hz is the high exponent in the New England Orogen, which distinguishes it from the Lachlan Orogen to the west. The Lachlan Belt shows relatively high Q, but the group velocities are rather slow toward the north, and faster in the south.

5.3. Ground-motion simulation

Observations of individual earthquakes provide only a limited sampling of ground motion at seismic stations, but we can combine our models of the Lg Q distribution with the assumed geometrical spreading (square root of epicentral distance) from a source to produce a ground motion pattern across the whole continent from any event. In effect we rebuild the Lg amplitude distribution based on the simple propagation model (1) used for the Q inversion.

In this way we are able to provide ground motion predictions for higher frequencies in regions that have not been directly sampled by earthquakes. Since the return period for continental earthquakes can be very long the absence of recorded earthquakes does not imply absence of earthquake hazard. Using the Lg Q distribution maps we can provide a direct indication of the main propagation effects from any event. The full ground-motion requires inclusion of source radiation effects and site effects, where known. After propagation for more than a hundred kilometres or so, the effects scattering by crustal heterogeneity tend to homogenise the radiation pattern. Amplification is to be expected above sedimentary basins, which contain many of the main population centres in Australia.

A number of Australian events have been felt at considerable distances from the source, and this can be explained by the efficient propagation of Lg through a high Q crust. In the Supplementary Material (Section S.5) we consider the Mw 6.6 event at Tennant Creek (20°S, 135°E) in 1998 that was felt from coast to coast. We show that the ground motion at the coast from this interior earthquake was equivalent to a local magnitude 2 (or larger) event and so could readily be felt with local sediment amplification, e.g. in the Perth basin.

With the continent wide consistent propagation model for Lg, we can investigate the decay of high frequency ground motion in a frequency band appropriate to resonances of large buildings and structures. This provides a useful new contribution to the assessment of seismic hazard across the Australian continent.

6. Conclusions

With the improved coverage of seismic datasets for Australia, we are able to provide Lg-wave attenuation models at different frequencies at good spatial resolution to provide useful constraints on crustal structure. The resulting tomographic images provide the supplementary information to map major tectonic boundaries, as well as further insights into the characteristics of different geology blocks for Australia.

(1) The study of the spatial decay of spectral amplitudes of Lg waves shows that the Lg-wave attenuation across the shield areas of the Australian continent is lower than for most other stable continents. The Phanerozoic zone has comparable attenuation to similar areas, such as eastern North America.
(2) The Lg Q maps display complex patterns of attenuation which generally correspond to the locations of sedimentary basins, orogenic belts, cratonic blocks and regions with high heat flow. There is a considerable difference in Lg attenuation in the crust between western Australia and eastern Australia. We find an attenuation strip in the eastern Australian crust that appears to be closely related to the Tasman line.
(3) The frequency dependence of Lg Q is not simply linear on a double-logarithmic scale, so the use of the commonly adopted power-law relationship across a broad span of frequencies is an over-simplification. In addition, the frequency dependence varies in different geological areas, with larger variations between tectonic provinces seen at higher frequencies (above 0.5 Hz).
(4) The combination of Lg Q, its frequency dependence, and the relative group velocity for Lg provide contrasting perspectives on the nature of the main crustal provinces across the continent. Strong gradients in properties generally have a close correspondence with mapped province boundaries, though they differ between the various characteristics of Lg.
(5) The Lg Q maps provide continent wide coverage of propagation effects for higher frequencies in the crust. They can be recombined with the assumed geometrical spreading relation to allow the assessment of the spread of energy for any event location as a contribution to understanding seismic hazard.

Acknowledgements

This work has been carried out at the Research School of Earth Sciences, Australian National University. The research was supported in large part by the China Scholarship Council (grant 201604910731) and the National Natural Science Foundation of China (grants 41374065 and 41674060), with additional support from the AuScope AuSREM project. We thank the IRIS Data Management Center (http://ds.iris.edu/ds/nodes/dmc) from which we extracted the waveform data, including the SKIPPY and KIMBA portable deployments made by ANU.

The images were drawn with Generic Mapping Tools version 5.2.1.

Appendix A. Supplementary data

Supplementary data to this article can be found online at http://dx.doi.org/10.1016/j.tecto.2017.08.022.

References

Atkinson, G.M., Mereu, R.F., 1992. The shape of ground motion attenuation curves in southeastern Canada. Bull. Seismol. Soc. Am. 82 (5), 2014–2031.

Benz, H.M., Frankel, A., Boore, D.M., 1997. Regional Lg attenuation for the continental United States. Bull. Seismol. Soc. Am. 87 (3), 606–619.

Bolt, B.A., 1957. Velocity of the seismic waves Lg and Rg across Australia. Nature 180, 495.

Bowman, J.R., Kennett, B.L.N., 1991. Propagation of Lg waves in the North Australian craton: influence of crustal velocity gradients. Bull. Seismol. Soc. Am. 81 (2), 592–610.

Cheng, H.X., Kennett, B.L.N., 2002. Frequency dependence of seismic wave attenuation in the upper mantle beneath the Australian region. Geophys. J. Int. 150 (1), 45–57.

Chow, R.A.C., Fairhead, J.D., Henderson, N.B., Marshall, P.D., 1980. Magnitude and Q determinations in southern Africa using Lg wave amplitudes. Geophys. J. Int. 63 (3), 735–745.

Clitheroe, G., Gudmundsson, O., Kennett, B.L.N., 2000. The crustal thickness of Australia. J. Geophys. Res. 105 (13) (697–13).

De Souza, J.L., Mitchell, B.J., 1998. Lg coda Q variations across South America and their relation to crustal evolution. In: In Q of the Earth: Global, Regional, and Laboratory Studies. Birkhäuser Basel, pp. 587–612.

Direen, N., Crawford, A.J., 2003. The Tasman line: where is it, what is it, and is it Australia's Rodinian breakup bounary? Aust. J. Earth Sci. 50, 491–502.

Erickson, D., McNamara, D.E., Benz, H.M., 2004. Frequency-dependent Lg Q within the continental United States. Bull. Seismol. Soc. Am. 94 (5), 1630–1643.

Furumura, T., Hong, T.K., Kennett, B.L.N., 2014. Lg wave propagation in the area around Japan: observations and simulations. Prog. Earth. Planet. Sci. 1 (1), 10.

Gregersen, S., 1984. Lg-wave propagation and crustal structure differences near Denmark and the North Sea. Geophys. J. Int. 79 (1), 217–234.

Gudmundsson, O., Kennett, B.L.N., Goody, A., 1994. Broadband observations of upper-mantle seismic phases in northern Australia and the attenuation structure in the upper mantle. Phys. Earth Planet. Inter. 84 (1), 207–226.

Hasegawa, H.S., 1985. Attenuation of Lg waves in the Canadian shield. Bull. Seismol. Soc. Am. 75 (6), 1569–1582.

Hill, D., 1951. In: Mack, G. (Ed.), Geology, in Handbook of Queensland. Aust. Assoc. for the Adv. of Sci., Brisbane, Queensland., Australia, pp. 13–24.

Issak, A., Camerlynck, C., 2016. Measuring crustal Lg-waves attenuation in the northern part of Africa. Open J. Earthq. Res. 5 (02), 105.

Jackson, I., Faul, U.H., 2010. Grainsize-sensitive viscoelastic relaxation in olivine: towards a robust laboratory-based model for seismological application. Phys. Earth Planet. Inter. 183 (1), 151–163.

Kennett, B.L.N., 1984. Guided wave propagation in laterally varying media—I. Theoretical development. Geophys. J. Int. 79 (1), 235–255.

Kennett, B.L.N., 1985. On regional-S. Bull. Seismol. Soc. Am. 75, 1077–1086.

Kennett, B.L.N., 1986. Lg waves and structural boundaries. Bull. Seismol. Soc. Am. 76 (4), 1133–1141.

Kennett, B.L.N., 2002. The Seismic Wavefield II: Interpretation of Seismograms on Regional and Global Scales. Cambridge University Press.

Kennett, B.L.N., Abdullah, A., 2011. Seismic wave attenuation beneath the Australasian region. Aust. J. Earth Sci. 58 (3), 285–295.

Kennett, B.L.N., Blewett, R.S., 2012. Lithospheric framework of Australia. Episodes 35 (1), 9–22.

Kennett, B.L.N., Fishwick, S., Reading, A.M., Rawlinson, N., 2004. Contrasts in mantle structure beneath Australia: relation to Tasman lines? Aust. J. Earth Sci. 51 (4), 563–569.

Kennett, B.L.N., Salmon, M., Saygin, E., AusMoho Working Group, 2011. AusMoho: the variation of Moho depth in Australia. Geophys. J. Int. 187 (2), 946–958.

Khazanehdari, J., Rutter, E.H., Brodie, K.H., 2000. High-pressure-high-temperature seismic velocity structure of the midcrustal and lower crustal rocks of the Ivrea-Verbano zone and Serie dei Laghi, NW Italy. J. Geophys. Res. Solid Earth 105 (B6), 13843–13858.

Knopoff, L., Schwab, F., Kauselt, E., 1973. Interpretation of Lg. Geophys. J. Int. 33 (4), 389–404.

Knopoff, L., Mitchel, R.G., Kausel, E.G., Schwab, F., 1979. A search for the oceanic Lg phase. Geophys. J. Int. 56 (1), 211–218.

Korsch, R.J., Doublier, M.P., 2016. Major crustal boundaries of Australia, and their significance in mineral systems targeting. Ore Geol. Rev. 76, 211–228(We acknowledge IRIS DMC http://ds.iris.edu/ds/nodes/dmc).

Mitchell, B.J., Pan, Y., Xie, J., Cong, L., 1997. Lg coda Q variation across Eurasia and its relation to crustal evolution. J. Geophys. Res. Solid Earth 102 (B10), 22767–22779.

Mitchell, B.J., Baqer, S., Akinci, A., Cong, L., 1998. Lg coda Q in Australia and its relation to crustal structure and evolution. Pure Appl. Geophys. 153 (2–4), 639–653.

Oliver, J., Ewing, M., 1957. Higher mode surface waves and their bearing on the Earth's mantle. Bull. Seismol. Soc. Am. 47, 187–204.

Paige, C.C., Saunders, M.A., 1982. LSQR: an algorithm for sparse linear equations and sparse least squares. ACM Trans. Math. Softw. 8 (1), 43–71.

Pasyanos, M.E., Matzel, E.M., Walter, W.R., Rodgers, A.J., 2009. Broad-band Lg attenuation modelling in the Middle East. Geophys. J. Int. 177 (3), 1166–1176.

Press, F., Ewing, M., 1952. Two slow surface waves across North America. Bull. Seismol. Soc. Am. 42 (3), 219–228.

Ruzaikan, A.I., Nersesov, I.L., Khalturin, V.I., Molnar, P., 1977. Propagation of *Lg* and lateral variation in crustal structure in Asia. Geophys. J. Int. 82, 307–316.

Salmon, M., Kennett, B.L.N., Stern, T., Aitken, A.R.A., 2013. The Moho in Australia and New Zealand. Tectonophysics 609, 288–298.

Saygin, E., Kennett, B.L.N., 2012. Crustal structure of Australia from ambient seismic noise tomography. J. Geophys. Res. Solid Earth 117 (B1).

Scheibner, E., Veevers, J.J., 2000. Tasman fold belt system. In: Veevers, J.J. (Ed.), Billion-Year Earth History of Australia and Neighbours in Gondwanaland. GEMOC Press, Sydney, N. S. W., Australia, pp. 154–234.

Sheehan, A.F., Torre, T.L., Monsalve, G., Abers, G.A., Hacker, B.R., 2014. Physical state of Himalayan crust and uppermost mantle: constraints from seismic attenuation and velocity tomography. J. Geophys. Res. Solid Earth 119 (1), 567–580.

Singh, C., Singh, A., Mukhopadhyay, S., Shekar, M., Chadha, R.K., 2011. Lg attenuation characteristics across the Indian shield. Bull. Seismol. Soc. Am. 101 (5), 2561–2567.

Yang, X., 2002. A numerical investigation of Lg geometrical spreading[J]. Bulletin of the Seismological Society of America 92 (8), 3067–3079.

Zhao, L.F., Xie, X.B., 2016. Strong Lg-wave attenuation in the Middle East continental collision orogenic belt. Tectonophysics 674, 135–146.

Zhao, L.F., Xie, X.B., Wang, W.M., Zhang, J.H., Yao, Z.X., 2010. Seismic Lg-wave Q tomography in and around Northeast China. J. Geophys. Res. Solid Earth 115 (B8).

Zhao, L.F., Xie, X.B., He, J.K., Tian, X., Yao, Z.X., 2013a. Crustal flow pattern beneath the Tibetan plateau constrained by regional Lg-wave Q tomography. Earth Planet. Sci. Lett. 383, 113–122.

Zhao, L.F., Xie, X.B., Wang, W.M., Zhang, J.H., Yao, Z.X., 2013b. Crustal Lg attenuation within the North China craton and its surrounding regions. Geophys. J. Int. 195 (1), 513–531.